Optical Biopsy of Amelanotic Melanoma with Raman and Autofluorescence Spectra Stimulated by 785 nm Laser Excitation

Ivan A. Bratchenko[1†], Yulia A. Khristoforova[1*], Lyudmila A. Bratchenko[1], Alexander A. Moryatov[2], Sergey V. Kozlov[2], Ekaterina G. Borisova[3], and Valery P. Zakharov[1]

[1] Samara National Research University, 34 Moskovskoe shosse, Samara 443086, Russia
[2] Samara State Medical University, 89 Chapaevskaya str., Samara 443099, Russia
[3] Bulgarian Academy of Sciences, 72 Tsarigradsko Chaussee Blvd, Sofia 1784, Bulgaria

† **e-mail:** iabratchenko@gmail.com

* **e-mail:** khristoforovajulia@gmail.com

I. A. Bratchenko and Y. A. Khristoforova should be considered joined first author

Abstract. In this work, Raman and autofluorescence spectroscopy in the near-infrared region has been used for examining amelanotic melanoma as the most dangerous type of malignant melanoma. There were 9 patients with amelanotic melanoma, 60 with pigmented melanoma and 120 with basal cell carcinoma enrolled in this study. We studied 9 amelanotic melanoma cases to differentiate them from basal cell carcinoma (n = 120) and pigmented malignant melanoma (n = 60) using portable spectroscopy setup with laser excitation source at 785 nm and low-cost spectrometer. The spectra of the different tumor type were classified using projection on the latent structure analysis with 10-Fold cross-validation. The results of the tumor classification were presented using box-plot diagrams and ROC analysis. We obtained 0.53 and 0.88 ROC AUCs for distinguishing amelanotic melanoma versus (1) pigmented melanoma and (2) basal cell carcinoma respectively based on the joint autofluorescence and Raman spectroscopy analysis that allowed one to diagnose amelanotic melanoma as true melanoma but no basal cell carcinoma.

Keywords: Raman spectroscopy; autofluorescence; optical biopsy; projection on the latent structure analysis; PLS; amelanotic melanoma; basal cell carcinoma; skin cancer.

Paper #3415 received 13 Apr 2021; revised manuscript received 22 Jun 2021; accepted for publication 25 Jun 2021; published online 30 Jun 2021. doi: 10.18287/JBPE21.07.020308.

1 Introduction

Melanoma is one of the most aggressive skin malignancies that caused the highest number of deaths of the all cases of skin cancer due to its metastatic character. In 2020, 324 635 new cases of melanoma incidence and 57 043 deaths from melanoma were registered worldwide that is significantly higher in comparison with the last years [1]. Moreover, a high incidence of melanoma is observed among young individuals in comparison with other skin tumors.

The ABCD algorithm is basic diagnostic method for melanoma detection at the preliminary stage worldwide based on the following features: asymmetry (A), border irregularity (B), color (C) variation and diameter (D). However, atypical morphological features of malignant melanoma (MM) complicate the detecting melanoma at the early stages that leads to the untimely treatment. Amelanotic melanoma (AMM) is one of the most dangerous melanoma types accounted for about 2–8% of all melanomas [2, 3]. AMM has a variety of clinical appearances and partial or complete pigment absence

simulating nonmelanocytic skin lesions (basal cell carcinoma (BCC), keratoacanthoma, seborrheic keratosis, Bowen's disease, etc.), that may not be so dangerous to the patient's survival as MM. Dermoscopy analysis is not effective to diagnose AMM as true MM, as no specific clinical features and histopathologic standards [3] correspond to the AMM. This greatly complicates the detecting of AMM at the early stages even for the most experienced oncologists.

Today, optical biopsy is one of the promising methods to detect tumors based on their spectral features caused by the contribution of the different chemical components. Different optical methods including terahertz spectroscopy [4], ultraviolet and visible fluorescence spectroscopy [5], Raman spectroscopy [6, 7], diffuse reflectance spectroscopy [9] demonstrated possibility to diagnose cancer of the different body sites and in particular skin cancer. However, to improve the efficiency of the optical biopsy to detect skin cancer the combination of the different methods may be used [9]. Some initial efforts in this direction are presented more than ten years ago, using combination of UV-excited autofluorescence and diffuse reflectance spectroscopy of pigmented skin disorders, including AMM lesions. However, the authors utilized 337 nm nitrogen laser as an excitation source, which is suboptimal for clinical applications, due to complex support of this type of laser systems and UV irradiation application [10].

When using long wavelength spectral range, namely 785 nm laser excitation for tissue analysis, one has a unique possibility to register simultaneously both autofluorescence in the near-infrared region (NIR) and Raman signals that carries information about biochemical composition of tissue [7]. In this context, combination of Raman and autofluorescence could be an appropriate method for recognizing AMM as a true MM at the preliminary step based on the specific spectral features.

Recent studies [6–8] have performed optical biopsy based on the Raman spectroscopy and/or autofluorescence analysis to classify melanoma versus seborrheic keratosis, pigmented nevus and other type of malignant tumors (BCC, squamous cell carcinoma). Zeng et al. [11] focused on the detection of the spectral differences between cancer and benign lesions using 785 nm Raman spectroscopy. Borisova et al. [12, 13] have studied pigmented melanoma and different types of malignant and benign pigmented tumors based on the ultraviolet, visible and NIR autofluorescence spectroscopy. Puppels et al. [14] demonstrated the power of Raman spectroscopy to differentiate melanoma from different type of pigmented nevi. These results are very valuable for the detecting of true pigmented MM, however, there is a lack of studies involving optical biopsy in AMM detection. Therefore, the aim of this work is the application of Raman and autofluorescence combination in the detection of AMM among other malignant tumors.

2 Materials and methods

2.1 Experimental setup

In vivo tumors spectra were registered using portable spectroscopic setup using NIR excitation source (785 nm laser diode), spectrometer QE 65Pro (Ocean Optics Inc.) and Raman optical probe InPhotonics [6]. Laser radiation 785 nm is delivered to the optical detector by excitation fibers (100 μm diameter, 0.22 NA) and collimating lenses. NIR (785 nm) laser radiation passes through the bandpass filter (BPF), which cuts off the Raman component of the optical fiber. The dichroic mirror transmits 785 nm laser radiation to lens, which focuses exciting radiation onto the sample (7 mm focal length). The same lens collects Raman signal, autofluorescence and backscattered radiation. The same dichroic mirror transmits the collected radiation to NIR channels, which include an appropriate longpass filter to cut off exciting NIR laser radiation, matching lens, and collection fibers (200 μm diameter, 0.22 NA), connected to spectrometer QE 65Pro.

The spectra were registered in the 780–1000 nm region in SpectraSuite program with 0.2 nm spectral resolution that was obtained using 200 μm slit in the spectrometer. The integration time of each spectrum was 20 s with triple accumulation. The silicon tip on the optical probe allowed one to fix the 7 mm distance between probe and the skin surface to obtain the collection of the scattered radiation from the upper skin layer of 1 to 2 mm from the different anatomical sites. The laser power density on the skin was about 0.3 W/cm^2 and did not caused any damage to the skin or discomfort in patients.

2.2 Materials

The protocols of the *in vivo* tissue diagnostics were approved by the ethical committee of Samara State Medical University (Samara Region, Samara, Russia, protocol No 132, 29 May 2013, clinical studies fall within The Code of Ethics of a Doctor of Russia, approved at the 4th conference of the Russian Medical Association, and within the World Medical Association Declaration of Helsinki). All patients were at least 18 years old. Informed consents were acquired from all patients before the *in vivo* study.

In total, 189 spectra skin neoplasms were registered *in vivo* using spectroscopic system from 189 patients (60 pigmented MM (PMM), 9 AMM and 120 BCC). Type of each tumor was identified using histopathological analysis.

2.3 Spectra preprocessing and data analysis

In vivo spectra statistical analysis was performed in 800–914 nm region that corresponds to the 237–1800 cm^{-1}. All spectra were smoothing by Savitzky-Golay filter (0 derivative order, 15 window width,

2 polynomial order), normalized on the standard deviation of the whole spectrum to reduce dispersion of experimental data and centered for further analysis.

The analyzed spectral region 237–1800 cm^{-1} contains both broadband autofluorescence signal and weak Raman peaks. However, autofluorescence overlaps weak Raman signal in the 237 to 1200 cm^{-1} region due to low signal-to-noise ratio (SNR) and only fluorescent skin features may be analyzed in this part of spectral region. In the 1200 to 1800 cm^{-1} range a smaller autofluorescence contribution is observed, which allows one extracting tissue Raman peaks from the registered signal. Thus, tissue Raman peaks are important features of the 1200 to 1800 cm^{-1} spectral range. Analysis of the entire spectrum of skin in the 237–1800 cm^{-1} takes into account both autofluorescence and Raman spectral features of analyzed tissues [6].

The entire spectra in the 800–914 nm area contain hidden links between different spectrum bands, due to the contribution of the same chemical components to these bands that causes multiple correlations of the spectral data. To analyze the highly correlated spectral data of the large dimension the regression analysis using the partial least square discriminant analysis (PLS–DA) was used [15]. PLS–DA method allows constructing the regression model for identifying spectra to the neoplasm classes based on the significant spectral differences by decomposing the original spectral data and the predictor matrix into a new space of lower dimension.

Four regression models were built in accordance with aim of this work:

(1) discrimination of PMM versus BCC;
(2) discrimination of PMM versus AMM;
(3) discrimination of all MM versus BCC;
(4) discrimination of AMM versus BCC.

The stability of the obtained classification PLS–DA models was checked by means of 10-fold cross-validation. The number of Latent Variables (LV) was chosen by the criterion of the minimum of the root mean square error (RMSE) for the applied of 10-Fold cross validation. We selected the first 4 (LVs) in (1) “PMM versus BCC” regression model, the first 3 LVs in (2) “PMM versus AMM” model, the first 2 LVs in both (3) “all MM versus BCC” and (4) “AMM versus BCC” models. The selected LVs describe 95% of the total variances of the spectral differences between analyzed tumor classes in (1) “PMM versus BCC” model, 94% in (2) “PMM versus AMM” model, 89% in (3) “all MM versus BCC” model and 86% in (4) “AMM versus BCC” model.

To determine the discriminant analysis of the analyzed neoplasm types, the PLS predictors were calculated to present the numeric value of the neoplasm diagnosis in the built model. PLS predictors were calculated in “R studio” software to implement the SIMPLS algorithm for PLS part of PLS–DA method using mdatools packages [16]. The PLS prediction algorithm is presented in Ref. [15]. Results of tumor classification based on the PLS analysis were presented using box-plot diagram and ROC curve. To quantify of the model’s efficiency, the area under the ROC curve (ROC AUC) was calculated.

3 Results and Discussion

Fig. 1 shows the mean spectra of PMM, AMM and BCC including Raman and autofluorescence signals with dispersion. The spectrum stimulated with 785 nm laser is a nonlinear decreasing autofluorescence curve with broadband maxima (near 870 nm) and narrow Raman peaks in 850–900 nm area. The broadband autofluorescence maxima that are contributed by the endogenous skin fluorophores (mainly melanin, lipids, lipofuscins and others [17]) overlap weak Raman bands especially near 866 nm (1200 cm^{-1}) that makes it difficult to register Raman signal in this spectral region, especially in MM analysis. Therefore, Raman bands can be visualized at wavenumbers between 1200 and 1800 cm^{-1}.

MM and BCC are skin malignancies with different biochemical and clinical features. According to the Fig. 1 the spectra of BCC and MM have distinguishable spectral differences both in the autofluorescence shape and in the intensity of the Raman signal. This allows one to perform classification of PMM (n = 60) and BCC (n = 120) with 0.95 accuracy (0.95 sensitivity and 0.96 specificity) and 0.98 ROC AUC (see Fig. 2 a, e). For BCC (n = 120) vs all MM (n = 69; including AMM and PMM) discriminating accuracy is 0.90 (0.86 sensitivity and 0.93 specificity) and AUC ROC is 0.86 (Fig. 2 b, f). Thus, addition of AMM to the analysis of MM and BCC lead to the decrease of the classification model performance. This fact may be explained by the low content of melanin both in AMM and BCC tissues.

As we can see from Fig. 1a, mean spectra of AMM and PMM have similar shape features of autofluorescence curve. Broadband maxima may be observed near 810, 840 and 865 nm. The spectral differences in the 800–870 nm region not exceed 5.9%. Both mean AMM and PMM spectra have spectral maxima at 840 and 865 nm in comparison with normal skin and other skin tumors such as BCC [12]. In our previous studies, we have mentioned that local maxima at 840 and 865 nm are observed in the spectra of tumors with high melanin concentration [12]. These peaks are shifted to longer wavenumber region that causes overlapping of Raman peaks at 1086 (υ_s (PO_2^-) in phospholipids), 1285–1305 cm^{-1} (υ_{as} (PO_2^-) in phospholipids and $\tau(CH_2)$ in collagen/phospholipids) in both PMM and AMM spectra.

The similar autofluorescence of PMM and AMM with different pigmentation level may be explained by contribution of multiple skin components. At the same time, high autofluorescence and broadband emission maxima in both PMM and nevi spectra are due to the high melanin concentration in these neoplasms [12]. Therefore, it is not clear which skin components besides melanin cause high autofluorescence during 785 nm laser stimulation of skin tissues. Darvin et al. [18] have examined the changes of the NIR autofluorescence and

Raman spectra for the different fraction of melanin at different depths in human skin using depth-resolved confocal microspectroscopy system. They found that NIR autofluorescence spectral characteristics are changed not rapidly while the melanin fraction changes. The main achievement of their study is that NIR autofluorescence in the skin is caused by the melanin, keratin and possible impact of proteins/lipids oxidation products. Thus, further studies are required in order to determine specific skin components that mostly contribute to AMM autofluorescence.

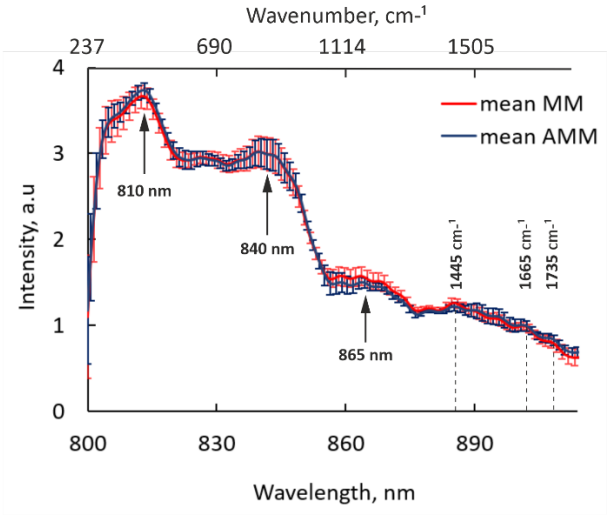

Fig. 1 The registered spectra of the skin neoplasms stimulated with 785 nm laser: (a) comparison of PMM and AMM spectra, (b) comparison of BCC and AMM.

AMM and BCC spectra are distinguished significantly with differences up to 54%. In comparison to AMM, BCC spectrum has decreasing curve with maximum values at 800–810 nm without broadband maxima at 840 and 865 nm. BCC mean spectrum are more smoothed in the region near 866 nm and allows one to register Raman peaks at 1285–1305 cm^{-1} ($\upsilon_{as}(PO_2^-)$ in phospholipids and $\tau(CH_2)$) in collagen/phospholipids, 1445 cm^{-1} ($\delta(CH_2)$ in lipids), 1665 cm^{-1} ($\upsilon(C=C)$ in unsaturated lipids, Amide I). Also, weak autofluorescence allows one to register Raman peak near 1086 cm^{-1} for some studied BCC.

Let us consider regression models based on spectral differences and similarities to separate AMM versus PMM and BCC. Table 1 and Fig. 2 (c–d, g–h) demonstrates the results for the built regression models. Fig. 2 (c, g) shows box-plot diagrams and ROC curve for the classification of PMM (n = 60) versus AMM (n = 9). The Fig. 2 (d, h) shows box-plot diagrams and ROC curve for the classification of AMM (n = 120) vs BCC (n = 9).

Table 1 Results of the tumor classification using PLS regression models.

Model		Accuracy	ROC AUC
PMM (n = 60) vs BCC (n = 120)		0.95	0.98
all MM (n = 69) vs BCC (n = 120)		0.90	0.86
PMM (n = 60) vs AMM (n = 9)	for 300–1800 cm^{-1}	0.75	0.53
	for 1200–1800 cm^{-1}	0.82	0.72
AMM (n = 9) vs BCC (n = 120)		0.90	0.88

The discrimination model of AMM vs PMM shows very poor result. The PLS predictors are equally concentrated in the narrow range of 0.10–0.16 relative units for both PMM and AMM spectra, and this fact significantly complicates AMM and PMM discrimination. The small variance of the PLS predictors for PMM and AMM spectra is caused by the small spectral differences. The ROC AUC of this model is only 0.53. The equivalent PLS predictors for PMM and AMM are caused by the similar biochemical compositions because any clinical subtype of cutaneous melanoma may be amelanotic [19]. In the case of AMM vs BCC we observe better results. The dispersion of the PLS predictors are in a wide range from 0.01 to 0.6 relative units. The obtained model allowed us to achieve 0.90 discrimination accuracy (0.89 sensitivity and 0.90 specificity) based on the joint Raman and autofluorescence analysis. The proposed optical biopsy approach demonstrates 0.88 ROC AUC for AMM and BCC separation.

The low discrimination of AMM and PMM is caused by similar broadband intensive autofluorescence, which mask low-intense Raman bands in the range of 237–1800 cm^{-1}. For typical MM, high autofluorescence is usually associated with increased melanin content in the tumor. In the case of AMM, there is a lack of accurate biochemical interpretation of studied tissues and

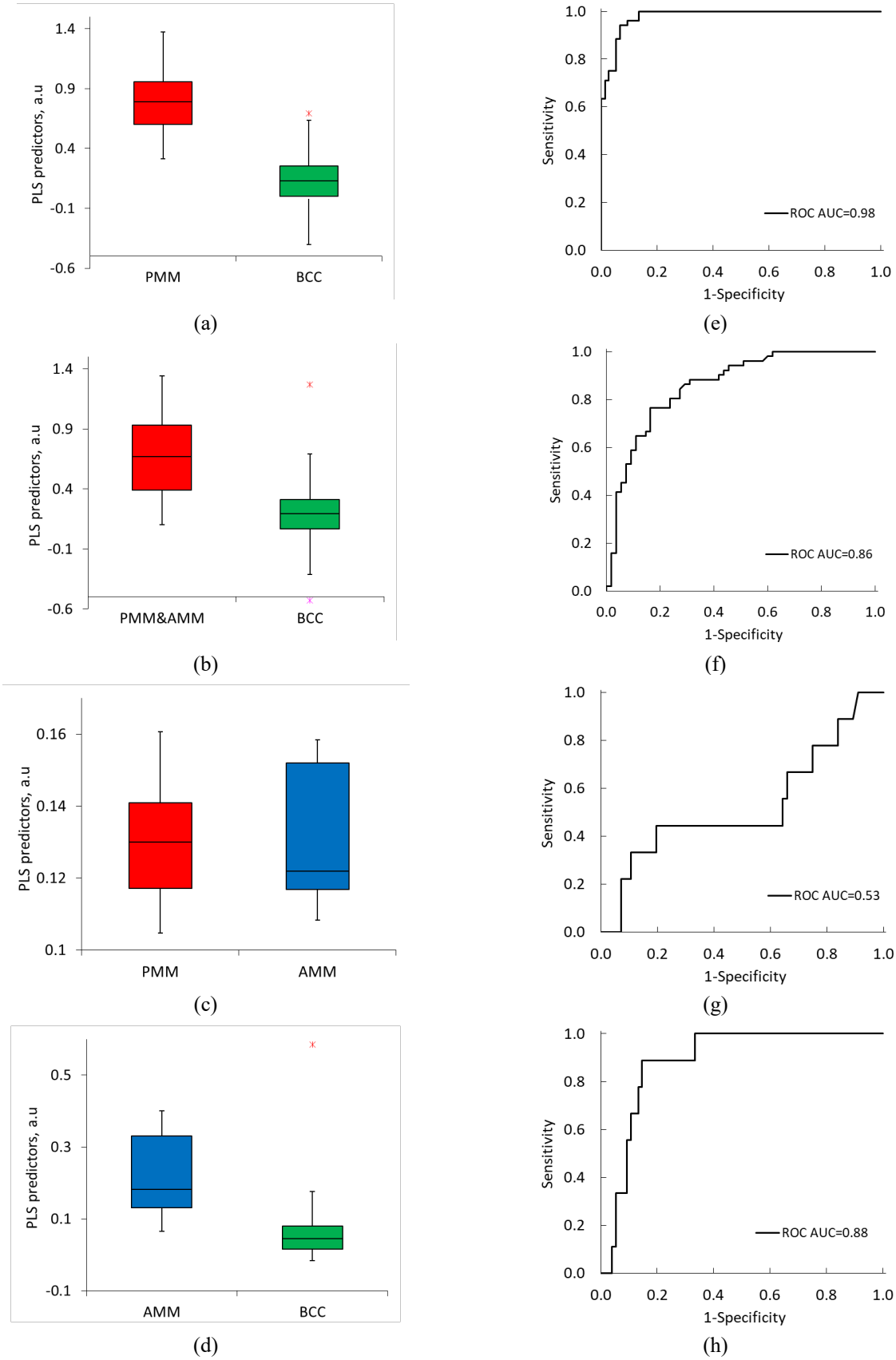

Fig. 2 Neoplasm classification by Raman and autofluorescence spectroscopy based on PLS-DA analysis: a–d Box-plots of PLS-predictors for discriminating skin lesions: (a) PMM vs BCC; (b) PMM & AMM vs BCC; (c) AMM vs PMM; (d) AMM vs BCC; e–h Corresponding ROC curves are derived from spreading PLS-predictors. Asterisks indicate outliers.

consequently along with the contribution of the melanin we may only assume the impact of other tissue components, such as proteins/lipids oxidation products [18]. This assumption may be partially confirmed by Meehan et al [3]. Their group had performed detailed morphologic analysis of 75 AMM cases and found that melanin might not be presented in AMM on visual inspection but it was detected on histopathological examination. In fact, PMM and AMM are subtypes of the same tumor type with similar composition of fluorophores but different relative concentrations, the total fluorescence spectrum of which is noninformative due to the overlap of the maxima. Therefore, for differentiation of PMM and AMM we completely removed fluorescence from registered spectra using baseline correction by asymmetric least squares method. This way allows us to perform classification of various melanoma types based only on Raman bands in the region 1200–1800 cm^{-1} with 0.82 accuracy (0.71 sensitivity and 0.85 specificity) and 0.72 ROC AUC. In accordance with Fig. 3 (a) PLS predictors medians for the PMM and AMM cohorts in box plot diagrams for this model are more differed in comparison with PLS predictors calculated when analyzing full tumor spectra in 237–1800 cm^{-1} region (Fig. 2 (c)) that results in improving classification accuracy to the 0.82. Therefore, we can assume that analysis of the Raman spectra is more effective for classification of different subtypes of melanoma in comparison with analysis of the full spectra containing both fluorescence and Raman signals because similar fluorescence features of AMM and PMM spectra do not allow to identify their Raman differences due to high overlap of their spectra.

In studies of skin cancer by Raman and autofluorescence spectroscopy several works have demonstrated promising results to classify MM versus other skin tumors. In such studies all cases of melanoma are considered as joint class without subtyping. Despite the importance of the AMM detection among all MM cases lack of works with AMM studying using optical methods is observed. Only in several medical studies selected cases of AMM were examined in details to demonstrate the difficulty of diagnosing AMM on the basis of only clinical or dermoscopic features [20, 21]. In different studies the misdiagnosed rate of AMM reaches a high value of 89% [21]. Cheung et al have investigated 75 AMM cases and only 2 cases demonstrated distinctive clinical features of AMM [3]. In study by Gualandri et al. only 2 cases of AMM (from 36 studied AMM cases in total) were suspected as true MM [2]. In study by Detrixhe et al. [22], it was shown that all 7 studied cases of AMM were incorrectly diagnosed by clinicians.

The obtained results show that spectral analysis in the NIR region allows one to define AMM as true MM. This finding is based on the similarity of AMM and PMM spectral properties. At the same time, it seems like AMM and MM differentiation is impossible based on the similar analysis of the full spectral region 237–1800 cm^{-1} and only Raman spectra in the 1200–1800 cm^{-1} can contain useful information to differ them. On the other hand, the real problem in clinical diagnosis is to differentiate AMM from other malignant tumors. In this study we achieved 0.90 accuracy and 0.88 ROC AUC in AMM and BCC separation. Such values of diagnostic performance are very promising and the proposed optical biopsy method may be helpful in clinical evaluation of AMM among nonmelanoma tumors. However, further large trials are required to prove this assumption.

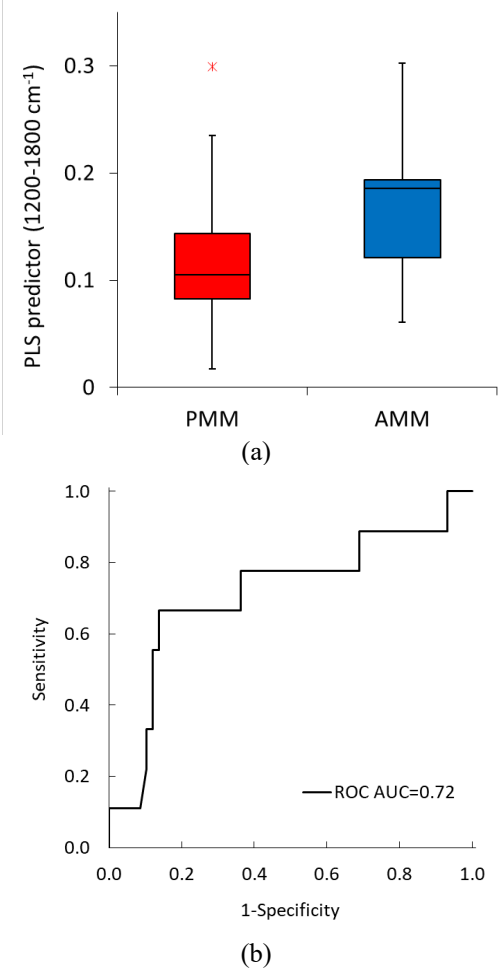

Fig. 3 PMM and AMM classification by Raman spectra in the 1200–1800 cm^{-1} based on PLS-DA analysis: (a) box-plots of PLS-predictors for discriminating skin lesions; (b) corresponding ROC curve is derived from spreading PLS-predictors. Asterisk indicates outlier.

4 Conclusions

AMM is the most dangerous type of MM because it either has been misdiagnosed frequently as BCC and other nonmelanotic benign lesions or not attract attention due to the absence of the clinical melanoma features. In result, AMM are progressed and detected at the advanced stages that is harmful to the patient's survival. In this work, we performed the classification of the AMM versus PMM and BCC cases. Spectral analysis on the basis of the near-infrared Raman and autofluorescence features allowed us to distinguish AMM and BCC with 0.90 accuracy while AMM and MM showed almost equal fluorescence spectral properties and only Raman signal

can contain useful spectral differences that can be proved by increase of the AMM cases. Achieved ROC AUC of AMM and BCC differentiation was 0.88 that proves the proposed technique of skin tumors optical biopsy may be useful in clinical practice. The obtained results show the power of spectral analysis to correctly define AMM as MM and avoid AMM treatment as other nonmelanoma tumors.

Disclosures

All authors declare that there is no conflict of interests in this paper.

Acknowledgments

This study is supported by joint program of Russian Foundation of Basic Research and Bulgarian Science Fund respectively under contracts № 19-52-18001 Bolg_a and № KP06-Russia/19/28.09.2019 "Multivariative Raman and fluorescence diagnosis of cutaneous tumors".

References

1. Global Cancer Observatory, Cancer Fact Sheets: Skin, 2020 (accessed 11 January 2021) [https://gco.iarc.fr/today/fact-sheets-cancers].
2. L. Gualandri, R. Betti, and C. Crosti, "Clinical features of 36 cases of amelanotic melanomas and considerations about the relationship between histologic subtypes and diagnostic delay," Journal of the European Academy of Dermatology and Venereology 23(3), 283–287 (2009).
3. W. L. Cheung, R. R. Patel, A. Leonard, B. Firoz, and S. A. Meehan, "Amelanotic melanoma: a detailed morphologic analysis with clinicopathologic correlation of 75 cases," Journal of Cutaneous Pathology 39(1), 33–39 (2012).
4. K. I. Zaytsev, K. G. Kudrin, V. E. Karasik, I. V. Reshetov, and S. O. Yurchenko, "In vivo terahertz spectroscopy of pigmentary skin nevi: Pilot study of non-invasive early diagnosis of dysplasia," Applied Physics Letters 106(5), 053702 (2015).
5. E. Borisova, T. Genova, V. Mircheva, P. Troyanova, I. Bratchenko, L. Bratchenko, Y. Khristoforova, V. Zakharov, I. Lihacova, A. Lihacovs, and J. Spigulis, "Multispectral fluorescence detection of pigmented cutaneous tumours," SPIE Proceedings 11585, 1158504 (2020).
6. I. A. Bratchenko, L. A. Bratchenko, A. A. Moryatov, Y. A. Khristoforova, D. N. Artemyev, O. O. Myakinin, A. E. Orlov, S. V. Kozlov, and V. P. Zakharov, "In vivo diagnosis of skin cancer with a portable Raman spectroscopic device," Experimental Dermatology 30(5), 652–663 (2021).
7. E. Cordero, I. Latka, C. Matthäus, I. W. Schie, and J. Popp, "In-vivo Raman spectroscopy: from basics to applications," Journal of Biomedical Optics 23(7), 071210 (2018).
8. L. A. Bratchenko, Y. A. Khristoforova, A. A. Morytatov, and I. A. Bratchenko, "Raman spectroscopy based diagnosis of dermatofibrosarcoma protuberans: Case report," Photodiagnosis and Photodynamic Therapy 35, 102351 (2021).
9. B. W. Murphy, R. J. Webster, B. A. Turlach, C. J. Quirk, C. D. Clay, P. J. Heenan, and D. D. Sampson, "Toward the discrimination of early melanoma from common and dysplastic nevus using fiber optic diffuse reflectance spectroscopy," Journal of Biomedical Optics 10(6), 064020 (2005).
10. E. Borisova, E. Nikolova, P. Troyanova, and L. Avramov, "Autofluorescence and diffuse reflectance spectroscopy of pigment disorders in human skin", Journal of Optoelectronics and Advanced Materials 10(3), 717–722 (2008).
11. H. Lui, J. Zhao, D. McLean, and H. Zeng, "Real-time Raman Spectroscopy for In Vivo Skin Cancer Diagnosis," Cancer Research 72(10), 2491–2500 (2012).
12. E. G. Borisova, I. A. Bratchenko, Y. A. Khristoforova, L. A. Bratchenko, T. I. Genova, A. I. Gisbrecht, A. A. Moryatov, S. V. Kozlov, P. P. Troyanova, and V. P. Zakharov, "Near-infrared autofluorescence spectroscopy of pigmented benign and malignant skin lesions," Optical Engineering 59(6), 061616 (2020)
13. E. Borisova, A. Gisbrecht, T. Genova-Hristova, P. Troyanova, E. Pavlova, N. Penkov, I. Bratchenko, V. Zakharov, I. Lihachova, I. Kuzmina, and J. Spigulis, "Multispectral autoflourescence detection of skin neoplasia using steady-state techniques," SPIE Proceeding 11047, 1104704 (2019).
14. I. P. Santos, R. van Doorn, P. J. Caspers, T. C. B. Schut, E. M. Barroso, T. E. Nijsten, V. N. Hegt, S. Koljenovic, and G. J. Puppels, "Improving clinical diagnosis of early-stage cutaneous melanoma based on Raman spectroscopy," British Journal of Cancer 119(11), 1339–1346 (2018).
15. D. M. Haaland, E. V. Thomas, "Partial least-squares methods for spectral analyses. 1. Relation to other quantitative calibration methods and the extraction of qualitative information," Analytical chemistry 60(11), 1193–1202 (1988).
16. S. Kucheryavskiy, "Mdatools: Multivariate Data Analysis for Chemometrics," R Package, version 0.9.4 (2019) [https://mdatools.com/].

17. I. Giovannacci, C. Magnoni, P. Vescovi, A. Painelli, E. Tarentini, and M. Meleti, "Which are the main fluorophores in skin and oral mucosa? A review with emphasis on clinical applications of tissue autofluorescence," Archives of Oral Biology 105, 89–98 (2019).
18. B. P. Yakimov, E. A. Shirshin, J. Schleusener, A. S. Allenova, V. V. Fadeev, and M. E. Darvin, "Melanin distribution from the dermal–epidermal junction to the stratum corneum: non-invasive in vivo assessment by fluorescence and Raman microspectroscopy," Scientific Reports 10(1), 14374 (2020).
19. M. Beyeler, R. Dummer, "Cutaneous melanoma: uncommon presentations," Clinics in Dermatology 23(6), 587–592 (2005).
20. M. Mascolo, D. Russo, M. Scalvenzi, S. Varricchio, and S. Staibano, "Pitfalls in the dermoscopic diagnosis of amelanotic melanoma," Journal of the American Academy of Dermatology 72(1), S2–S3 (2015).
21. H. Z. Gong, H. Y. Zheng, and J. Li, "Amelanotic melanoma," Melanoma Research 29(3), 221–230 (2019).
22. A. Detrixhe, F. Libon, M. Mansuy, N. Nikkels-Tassoudji, A. Rorive, J. E. Arrese, P. Quatresooz, M.-A. Reginster, and A. F. Nikkels, "Melanoma masquerading as nonmelanocytic lesions," Melanoma Research 26(6), 631–634 (2016).